

K-shell ionization of Al and Cu for 0.5-40-MeV-proton bombardment

著者	石井 慶造
journal or publication title	Physical review. A
volume	21
number	5
page range	1412-1418
year	1980
URL	http://hdl.handle.net/10097/35216

doi: 10.1103/PhysRevA.21.1412

K-shell ionization of Al and Cu for 0.5–40-MeV-proton bombardment

K. Sera and K. Ishii

Cyclotron and Radioisotope Center, Tohoku University, Sendai, 980 Japan

M. Kamiya, A. Kuwako, and S. Morita

Department of Physics, Faculty of Science, Tohoku University, Sendai, 980 Japan

(Received 5 September 1979)

K-shell ionization cross sections of Al and Cu for proton impact have been measured over the projectile-energy range 0.5–40 MeV, and the results are compared with calculations of plane-wave Born approximation (PWBA) and binary-encounter approximation (BEA). In the PWBA calculation, contributions from close and distant collisions are separately estimated by an approximate calculation. It is found that the distant collisions make a predominant contribution in the high-projectile-energy region and the experimental results are in better agreement with the PWBA than the BEA, which takes into account only the close collision.

I. INTRODUCTION

K-shell ionizations in the energy region $E/\lambda U < 1$, (where E is the projectile energy, λ is the ratio of the projectile mass to the electron mass, and U is the ionization energy of the target atom) have been extensively studied by many researchers, and it has been well established that the increased-binding-energy effect and Coulomb deflection play an important role in the ionization process.¹ On the other hand, systematic measurements of the ionization process in the high-energy region of $E/\lambda U > 1$ are still scarce.²⁻⁸ Inner-shell ionization is theoretically divided into that produced by close collisions and by distant collisions. The former process is calculated by the Rutherford scattering between the projectile and free electrons of velocity distribution corresponding to the inner-shell electrons, and the latter process is treated as the photoionization process by virtual photons produced by the projectile. It is expected from the results of Ref. 3 that in the low-energy region of $E/\lambda U < 1$, close collisions are the primary contribution to the ionization, whereas in the high-energy region of $E/\lambda U > 1$, distant collisions also become effective. Thus it must be worthwhile to measure the inner-shell ionization cross section in the high-energy region and to study the contributions from both close and distant collisions.

In the present work, K-x-ray production cross sections of Al and Cu for proton impact have been measured over the energy range 0.5–40 MeV. The ionization cross sections were obtained using the values of fluorescence yield given by Bambyneck *et al.*,⁹ and the experimental results are compared with calculations of plane-wave Born approximation (PWBA) and binary-encounter approximation

(BEA). In the PWBA calculation, the ionization cross sections for close collisions are approximately separated from those for distant collisions by utilizing the behavior of generalized oscillator strength for these two kinds of collisions.

II. EXPERIMENTAL

Aluminum and copper were chosen as target atoms, since the relativistic effect of orbital electrons can be neglected in comparing it with theoretical calculations. Thicknesses of these self-supporting targets were measured by the Rutherford scattering of protons to be 100 $\mu\text{g}/\text{cm}^2$ for Al and 32 $\mu\text{g}/\text{cm}^2$ for Cu. The Van de Graaff generator of our university was used to produce protons of energy 0.5–3 MeV and the newly built 680-type cyclotron of Sumitomo-CGR-MeV Inc. was used to produce 3–40-MeV protons. The proton beam extracted from the cyclotron was deflected by 15° with the first switching magnet in the cyclotron vault, and was again deflected by 35° with the second switching magnet in the magnet room as shown in Fig. 1. After passing through a concrete wall of 1-m thickness and also a heavy concrete shield of 50-cm thickness between the magnet room and the target room, the beam entered the target chamber, and then it was focused by a pair of quadrupole magnets on the end of a Faraday cup, which is 5.60 m from the target and is shielded with 100-cm-thick, heavy concrete blocks in order to reduce the background of nuclear γ rays from the Faraday cup. The beam duct consists of stainless-steel tube of 10-cm inner diameter.

K-x rays of Al and Cu were measured with a proportional counter, and an Ortec Si(Li) detector

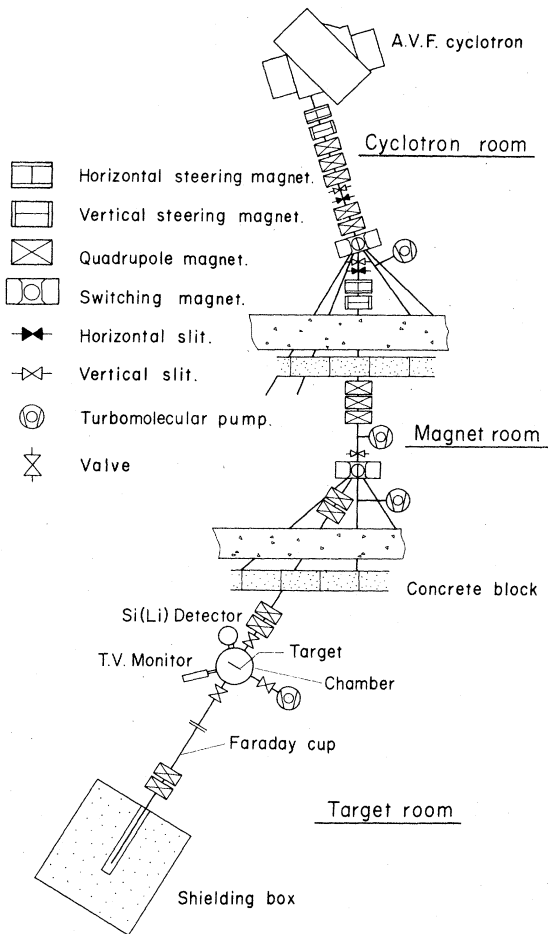


FIG. 1. Arrangement for the cyclotron experiment. In order to reduce the background due to nuclear γ rays, the target chamber and the detector are heavily shielded from the beam-switching magnet and the Faraday cup, and no slit is used in the target room.

with an energy resolution of 160 eV for 6.4-keV x-rays. The calibration and efficiency measurements of the detectors have already been reported^{10,11} and the results for Al obtained with the Van de Graaff generator have also been reported.¹¹ K-x-ray spectra of Al and Cu obtained from 40-MeV-proton bombardments with the cyclotron are shown in Fig. 2, where the backgrounds are quite small compared with the K-x-ray peaks.

The x-ray production cross sections obtained for Al and Cu are shown in Table 1. The accuracy of these cross sections is estimated to be 12% from the following errors: background subtraction, 2%; target thickness, 5%; counting statistics, 1%; and the detector efficiency and absorption correction, 11%.

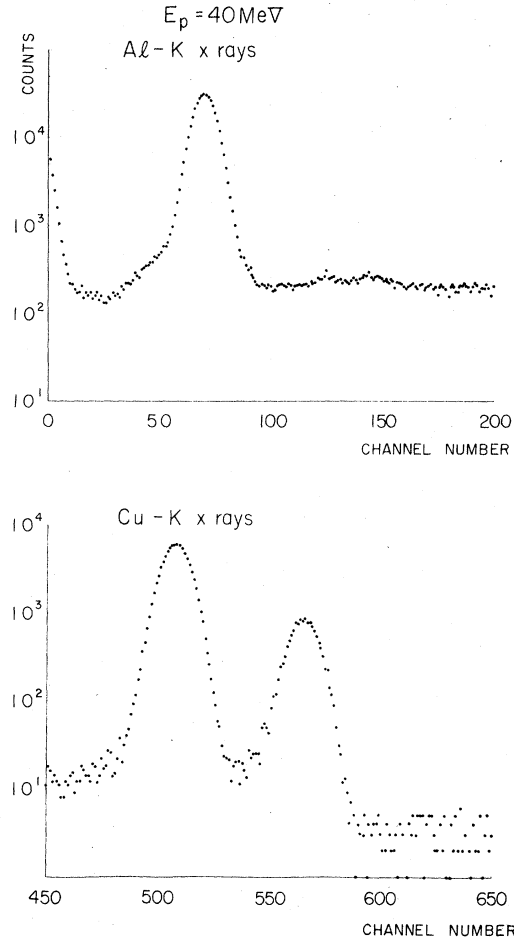


FIG. 2. K-x-ray spectra of Al and Cu produced by 40-MeV-proton impact.

III. PWBA CALCULATIONS

The PWBA calculation of inner-shell ionization by heavy-charged particles was first carried out by Bethe¹² using the dipole approximation, and has been developed by many authors.¹³⁻¹⁶ The BEA and semiclassical approximation (SCA) theories have been calculated by Garcia¹⁷ and by Hansteen and Mosebakk,¹⁸ respectively. In the BEA theory, orbital electrons of the target atom are considered to be free electrons of the same velocity distribution as the orbital ones, and the ionization is assumed to occur by the Rutherford scatterings between the projectile and the electrons, i.e., close collisions. Besides these collisions, the inner-shell ionization can also be produced by the distant collision, which results from the photoelectric effect of virtual photons produced by the projectile. In this section, the contribution of these

TABLE I. K -x-ray production cross section of Al and Cu for proton bombardment.^a

E_p (MeV)	Al σ_X^K (barn)	Cu σ_X^K (barn)
0.5		0.699
0.625		1.35
0.75	296	2.47
0.875		3.95
1.00	478	6.01
1.25	616	11.9
1.50	698	19.3
1.75		29.2
2.00	810	39.5
2.25		54.7
2.50	947	68.5
2.75		84.1
3.00	993	97.0
2.985	969	92.2
3.94	992	145
6.07	879	246
9.13	733	350
12.21	613	406
18.29	469	423
23.98	394	412
30.13	342	396
35.61	297	374
39.56	277	356

^aThe data from 0.5–3.00 MeV were obtained with the Van de Graaff generator, and those from 2.985–39.56 MeV were obtained with the cyclotron.

two kinds of collision to the total ionization is separately estimated in terms of the PWBA calculation.

In accordance with the nonrelativistic PWBA theory, the inner-shell ionization cross section is expressed by¹³

$$\begin{aligned} \sigma_{n',n} &= \frac{1}{2\pi} \frac{1}{\hbar^2 v^2} \int q dq \left| \int \psi_n^*(\vec{r}) \frac{ze^2 e^{i\vec{q}\cdot\vec{R}}}{|\vec{R}-\vec{r}|} \psi_{n'}(\vec{r}) d\vec{r} d\vec{R} \right|^2 \\ &= 8\pi z^2 \left(\frac{e^2}{\hbar v} \right)^2 \int \frac{dq}{q^3} \left| \int \psi_n^* e^{i\vec{q}\cdot\vec{r}} \psi_n d\vec{r} \right|^2, \end{aligned} \quad (1)$$

$$\sigma_n = 8\pi z^2 \frac{a_0^2}{Z_s^4} \frac{1}{\eta} \int \frac{dW}{W} \int \frac{dQ}{Q} F_n(W, Q). \quad (2)$$

Here z is the atomic number of the projectile, $\hbar q$ is the transfer momentum of the projectile and W is the transfer energy in units of the K -shell ionization potential $Z_s^2 R_y$; $W = k^2 + 1$ with the wave number of the ejected electron k , and Q and η are defined by

$$Q = \frac{\hbar^2 q^2}{2M} \frac{1}{Z_s^2 R_y}$$

and

$$\eta = \frac{1}{\lambda} \frac{E_p}{Z_s^2 R_y}.$$

The generalized oscillator strength $F_n(W, Q)$ in Eq. (2) is defined by¹²

$$F_n(W, Q) = \frac{W}{Q} \left| \int \psi_n^* e^{i\vec{q}\cdot\vec{r}} \psi_n d\vec{r} \right|^2, \quad (3)$$

and for the K shell it is given by¹⁹

$$\begin{aligned} F_K(W, Q) &= 2^7 W (Q + \frac{1}{2} W) [(W - Q)^2 + 4Q]^{-3} \\ &\quad \times [1 - \exp(-2\pi/k)]^{-1} \\ &\quad \times \exp\left(-\frac{2}{k} \tan^{-1} \frac{2k}{Q - k^2 + 1}\right). \end{aligned} \quad (4)$$

The final states in this calculation have been taken as continuum. Discussions hereafter are confined to the K -shell ionization. The generalized oscillator strength has been characterized by the Bethe surface,¹⁹ and it is divided into two regions in the transfer-momentum space as seen in Fig. 3, where $F_K(W, Q)$ is shown as a function of $\ln Q$ taking the transfer energy W as a parameter. As this figure shows, $F_K(W, Q)$ is flat in the region of low-transfer momentum, and at high-transfer momentum near $Q = W$ it reveals a peak known as the Bethe ridge.¹⁹ The plateau in the low- Q region comes from the fact that $F_K(W, Q)$ is approximated by an optical oscillator strength and the ionization is produced by the photoelectric effect, namely, distant collisions. On the other hand, if we assume free electrons of velocity distribution of K -

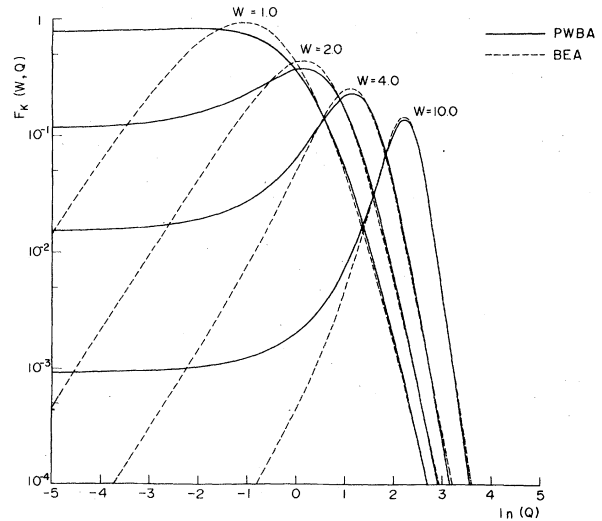


FIG. 3. The generalized oscillator strength for K shell $F_K(W, Q)$ obtained from PWBA and BEA is shown as a function of $\ln Q$; W and Q are the transfer energy and the transfer momentum, respectively.

shell electrons for the initial state in Eq. (3), the generalized oscillator strength is expressed by²⁰

$$F_K^{\text{BEA}}(W, Q) = 2^8 (3\pi)^{-1} W Q^{3/2} [(W - Q)^2 + 4Q]^{-3}, \quad (5)$$

on which the BEA theory is based. Dashed curves in Fig. 3 represent $F_K^{\text{BEA}}(W, Q)$, and it is seen that, in the high- Q region, $F_K^{\text{BEA}}(W, Q)$ corresponds to $F_K(W, Q)$ given by Eq. (4). Thus the generalized oscillator strength can be divided into two regions corresponding to the two kinds of ionization process. It must be noted, however, that the $F(W, Q)$ itself cannot be readily divided into two terms corresponding to the two kinds of collisions, because these two kinds are induced by the same interaction in the PWBA theory and are treated as a single process, whereas they are distinguished only from a point of view of classically based kinematics. Hence, the ionization cross section cannot exactly, but only approximately, be separated into two terms corresponding to the two processes as discussed below.

The ionization cross section σ^i of Eq. (2) given by W - Q representation can also be expressed by the impact-parameter representation, SCA, and if we define collisions of impact-parameter b smaller than the orbital radius of the electron a as close collisions and those of $b > a$ as distant collisions,²¹ then the ionization cross sections, σ^{CC} and σ^{DC} , corresponding to close and distant collisions, respectively, can be calculated by

$$\begin{aligned} \sigma^{\text{CC}} &= \int_0^a p(b) 2\pi b db, \\ \sigma^{\text{DC}} &= \int_a^\infty p(b) 2\pi b db. \end{aligned} \quad (6)$$

However, this distinction based on the *domain of collision* is not equivalent to the classification which we here look for: close collisions due to the Rutherford scattering and distant collisions due to the photoelectric effect.

Corresponding to the distinction of Eq. (6), a similar separation in the W - Q space can be considered. In conformity with scattering theory, the transfer momentum q is related to the radius of scatterer a by $qa > 1$, and the scattering can be described by the classical approximation.²² Taking a as the orbital radius of inner-shell electrons, this condition becomes $Q > 1$. Thus, in the Q integration of Eq. (2) of the PWBA calculation, the ionization cross section can be divided into the regions of $Q > 1$ and $Q < 1$, corresponding to close and distant collisions, respectively.

As seen in Fig. 3, however, this distinction is not valid in the region of high-transfer energy, where the process behaves as distant collisions even in the region of $Q > 1$. Thus, the separation

of the ionization cross section into the two parts cannot appropriately be done on the basis of the domain of collision nor on the kinematic space. Hence, a separation is tried here on the basis of a formula from impulse approximation (BEA) for close collisions and a formula from dipole approximation for distant collisions.

The function $F_K^{\text{BEA}}(W, Q)$ given by Eq. (5) is chosen as the basic function for the separation, since $F_K^{\text{BEA}}(W, Q)$ was derived from close-collision approximation and shows the behavior of only close collisions in the whole region of W - Q space. As seen in Fig. 3, $F_K(W, Q)$ almost agree with $F_K^{\text{BEA}}(W, Q)$ in the region $Q \geq W$, and the term $F_K^{\text{CC}}(W, Q)$ corresponding to close collisions in $F_K(W, Q)$ can be taken as $F_K(W, Q)$ itself, namely,

$$F_K^{\text{CC}}(W, Q) = F_K(W, Q), \quad \text{for } Q \geq W. \quad (7)$$

By comparison of Eq. (4) with Eq. (5) and also from the behavior of Eq. (5) for small Q , the following function $F_K^{\text{DC}}(W, Q)$ is tentatively chosen:

$$\begin{aligned} F_K^{\text{DC}}(W, Q) &= 2^7 W \frac{4}{3} Q [(W - Q)^2 + 4Q]^{-3} \\ &\times [1 - \exp(-2\pi/k)^{-1}] \\ &\times \exp\left(-\frac{2}{k} \tan^{-1} \frac{2k}{Q - k^2 + 1}\right), \quad \text{for } Q \leq W. \end{aligned} \quad (8)$$

The functions $F_K^{\text{CC}}(W, Q)$ and $F_K^{\text{BEA}}(W, Q)$ are compared in Fig. 4, showing a good agreement with each other over the entire range of W - Q space. Thus, it is shown that $F_K^{\text{CC}}(W, Q)$ can be taken as

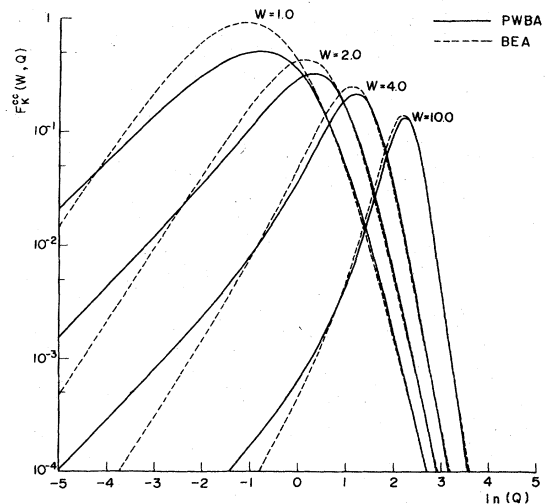


FIG. 4. The function $F_K^{\text{CC}}(W, Q)$ given by Eqs. (7) and (8) in the text is compared with the generalized oscillator strength of the BEA.

the term corresponding to close collisions. The term $F_K^{\text{DC}}(W, Q)$ corresponding to distant collisions can be derived from $F_K(W, Q) = F_K^{\text{DC}}(W, Q) + F_K^{\text{CC}}(W, Q)$ and Eqs. (5), (7), and (8), and is given by

$$F_K^{\text{DC}}(W, Q) = 2^7 W^{\frac{1}{3}} (W - Q) [(W - Q)^2 + 4Q]^{-3} \\ \times [1 - \exp(-2\pi/k)^{-1}] \\ \times \exp\left(-\frac{2}{k} \tan^{-1} \frac{2k}{Q - k^2 + 1}\right), \text{ for } Q \leq W$$

and

$$F_K^{\text{DC}}(W, Q) = 0, \text{ for } Q \geq W. \quad (9)$$

The functions $F_K^{\text{CC}}(W, Q)$ and $F_K^{\text{DC}}(W, Q)$ thus obtained are represented in Fig. 5 together with $F_K(W, Q)$. As seen in this figure, $F_K^{\text{DC}}(W, Q)$ agrees with the optical oscillator strength in the small- Q region.

By using $F_K^{\text{DC}}(W, Q)$ and $F_K^{\text{CC}}(W, Q)$, K -shell ionization cross sections corresponding to distant collisions σ_K^{D} and to close collisions σ_K^{C} are expressed by

$$\sigma_K^{\text{D}} = 8\pi z^2 \frac{a_0^2}{Z_s^4} \frac{1}{\eta} \int_0^\infty \frac{dW}{W} \int_{W^2/4\eta}^\infty \frac{dQ}{Q} F_K^{\text{DC}}(W, Q), \quad (10)$$

$$\sigma_K^{\text{C}} = 8\pi z^2 \frac{a_0^2}{Z_s^4} \frac{1}{\eta} \int_0^\infty \frac{dW}{W} \int_{W^2/4\eta}^\infty \frac{dQ}{Q} F_K^{\text{CC}}(W, Q). \quad (11)$$

The total cross section and σ_K^{D} and σ_K^{C} for the K -shell ionization of Al by proton impact are shown in Fig. 6 together with the BEA calculation. The

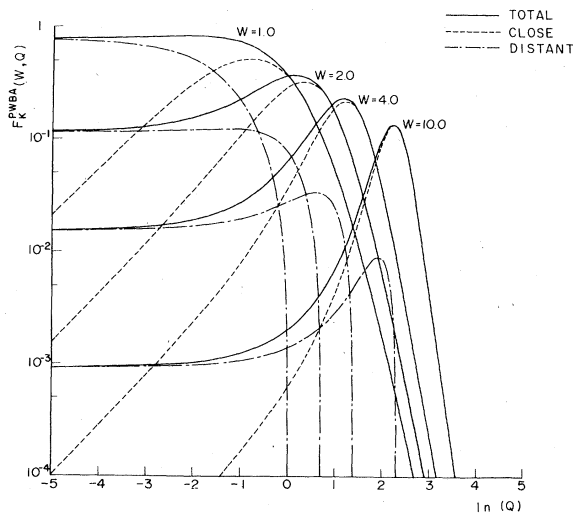


FIG. 5. The generalized oscillator strength $F_K^{\text{PWBA}}(W, Q)$ is divided into the dashed lines, $F_K^{\text{CC}}(W, Q)$ and the dot and dashed lines, $F_K^{\text{DC}}(W, Q)$ corresponding to close and distant collisions, respectively.

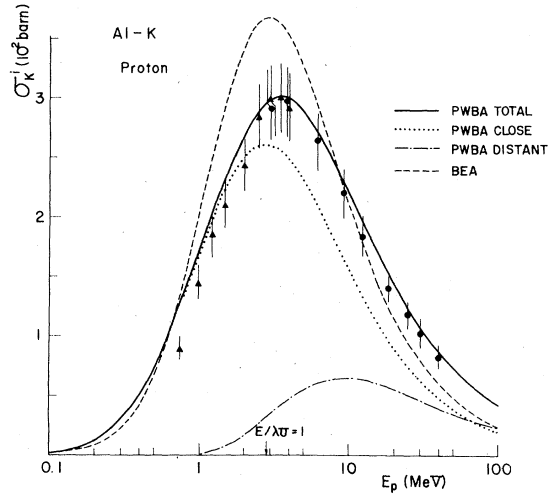


FIG. 6. Theoretical calculations for the K -shell ionization of Al by proton impacts are compared with the experimental results. The dotted and the dot and dashed curves, respectively, stand for the cross sections of close and distant collisions, σ_K^{C} and σ_K^{D} . The triangles were obtained with the Van de Graaff generator and the circles were with the cyclotron.

cross section σ_K^{C} has a maximum at $E/\lambda U = 1$ in accordance with the BEA theory, and this fact is a characteristic feature of close collisions. In the region $E/\lambda U < 1$, almost all of the ionizations are due to close collisions; in the region $E/\lambda U > 1$, distant collisions also become effective and as the incident energy gets higher, both collisions contribute equally to the ionization. The fact that the projectile energy corresponding to the maximum cross section given by the PWBA is larger than $E = \lambda U$ is due to the contribution from distant collisions. At very high-projectile energy where the relativistic treatment is needed, the transverse parts of the electromagnetic interaction between the projectile and the inner-shell electron, which have been neglected in the present calculation, become effective.²³

IV. COMPARISONS BETWEEN EXPERIMENT AND THEORIES

Using the values of fluorescence yield $\omega_K = 0.0333$ and 0.445 for Al and Cu, respectively,⁹ ionization cross sections were obtained from the x-ray production cross sections. The experimental results, obtained over the incident energy region $E/\lambda U = 0.1746$ –11.179 for Al and 0.0303–1.94 for Cu, are shown in Figs. 6 and 7, together with the results predicted from the PWBA and BEA theories. Besides the present experimental results,

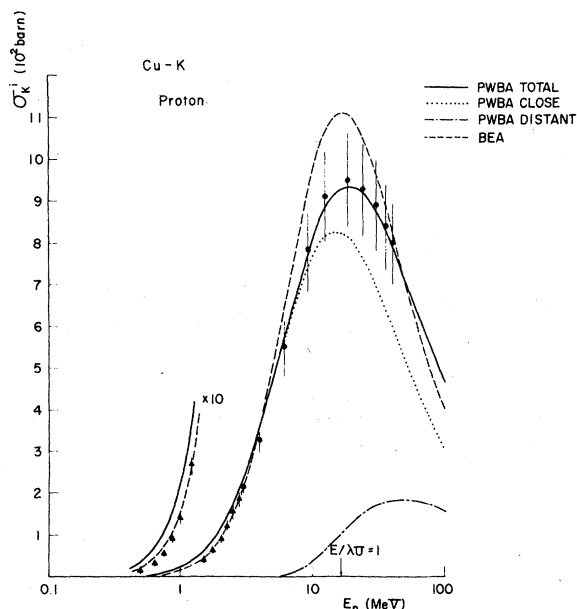


FIG. 7. Same as Fig. 4 except for Cu.

K -shell ionization cross sections of Al and Cu for proton impact have been reported by Garcia *et al.*,²⁴ Basbas *et al.*,¹ Tawara *et al.*,¹¹ and Basbas *et al.*⁷ Earlier data were mostly deduced from thick-target x-ray yield with large uncertainties of about 20% or more and obtained in the proton-energy region below ~ 5 MeV, except the work of Basbas *et al.*,⁷ which deals with the data in the energy region 0.01–10 MeV/amu. Only the present results are shown in Figs. 6 and 7, since our results are in agreement with the others, particularly in excellent agreement with those of Basbas *et al.*, within the experimental error in the overlapping energy regions. Furthermore, our main interest here is focused on the high-energy region.

In the region $E/\lambda U < 1$, the experimental results for Al are smaller than the theories,⁷ while those for Cu are in good agreement with theories. In the region of $E/\lambda U \approx 1$, the experimental cross sections for both Al and for Cu agree well with the PWBA, while the BEA is considerably higher.²⁴ This behavior corresponds to the fact that the generalized oscillator strength given by the BEA is larger than that of the PWBA, as seen in Fig. 3. However, in the low-energy region, where the minimum momentum transfer becomes large, the situation is just the opposite. The experimental K -shell ionization cross sections for Al in the energy region $E/\lambda U > 1$ agree well with the predictions from the PWBA. From the point of view

of the PWBA, distant and close collisions are expected to contribute approximately equally in this energy region. Our present experimental results are in good agreement with PWBA rather than with the BEA.

According to Bissinger *et al.*,⁴ a value of screening constant θ_K smaller than the relativistic one is needed to obtain an agreement with the PWBA, while in our case the relativistic value does not agree with the experiment, especially in the region $E/\lambda U \approx 1$, representing no contradiction to the theory.

A systematic deviation of experimental results from the PWBA calculation has been reported by Bissinger *et al.*³ in the case of C K -shell ionization with protons of $E/\lambda U > 1$, and they pointed out that this discrepancy would probably be due to use of unrealistic wave functions for the inner-shell electron. In our case of Al, however, no such discrepancy is found and it seems that a hydrogenlike wave function is plausible. On the other hand, the discrepancy reported by Bissinger *et al.*³ may be understood in terms of interference effect between the first and the second Born terms calculated by Reading *et al.*²⁵ In our case, however, this interference effect is supposed to be negligible because of the fact that this effect is about 4% in the experimental results obtained by Basbas *et al.*⁷ on the proton and He-ion bombardments of Al at $E/\lambda U = 2.6$ and from the projectile-energy dependence of the effect—inversely proportional to the projectile velocity—given by Reading *et al.*²⁵

The K -shell ionization in a region of intermediate-projectile velocities has been discussed extensively by Basbas *et al.*⁷: They analyzed the contributions from various effects such as the charge transfer process and the polarization effect. In the present work, however, these contributions are smaller than the experimental errors of 12%, since the projectiles are protons, and these effects are not discussed here.

V. SUMMARY

K -shell ionization cross sections of Al and Cu for proton impact have been obtained from x-ray measurements over the proton-energy range 0.5–40 MeV. The results were compared with the theories of BEA and PWBA. Taking the BEA theory as a basic close-collision approximation and dividing the generalized oscillator strength of the PWBA into two parts corresponding to close and distant collisions, the ionization cross section from PWBA was separated into contributions

from these two kinds of collisions. The good agreement between the experimental results and the PWBA theory, especially in the high-energy region of $E/\lambda U > 1$, reveals the important contribution from distant collisions in this region.

ACKNOWLEDGMENTS

We would like to thank Mr. Hoshika, Mr. Ohmura, and Mr. Ono for operation of the cyclotron throughout the experiment.

-
- ¹G. Basbas, W. Brandt, and R. Laubert, *Phys. Rev. A* **7**, 983 (1973).
²G. Bissinger, J. M. Joyce, and H. W. Kugel, *Phys. Rev. A* **14**, 1375 (1976).
³G. Bissinger, J. M. Joyce, B. L. Doyle, W. W. Jacobs, and S. M. Shafroth, *Phys. Rev. A* **16**, 443 (1977).
⁴G. A. Bissinger, J. M. Joyce, E. J. Ludwig, W. S. McEver, and S. M. Shafroth, *Phys. Rev. A* **1**, 841 (1970).
⁵T. L. Hardt and R. L. Watson, *Phys. Rev. A* **7**, 1917 (1973).
⁶W. D. Ramsay, M. S. A. L. Al-Ghazi, J. Birshall, and J. S. C. McKee, *Phys. Lett.* **69A**, 258 (1978).
⁷G. Basbas, W. Brandt, and R. Laubert, *Phys. Rev. A* **17**, 1655 (1978).
⁸M. Poncet and Ch. Engelmann, *Nucl. Instrum. Methods* **159**, 455 (1979).
⁹W. Bambynek, B. Crasemann, R. W. Fink, H. U. Freund, H. Mark, C. D. Swift, R. E. Price, and P. V. Rao, *Rev. Mod. Phys.* **44**, 716 (1972).
¹⁰H. Tawara, K. Ishii, S. Morita, H. Kaji, C. N. Hsu, and T. Shiokawa, *Phys. Rev. A* **9**, 1617 (1974).
¹¹H. Tawara, Y. Hachiya, K. Ishii, and S. Morita, *Phys. Rev. A* **13**, 572 (1976).
¹²H. Bethe, *Ann. Phys. (Leipzig)* **5**, 325 (1930).
¹³E. Merzbacher and H. W. Lewis, *Handbuch der Physik* edited by S. Flügge (Springer, Berlin, 1958), Vol. **34**, p. 166.
¹⁴G. H. Choi, *Phys. Rev. A* **4**, 1002 (1971).
¹⁵B. H. Choi, E. Merzbacher, and G. S. Khandelwal, *At. Data* **5**, 291 (1973).
¹⁶B. H. Choi, *Phys. Rev. A* **7**, 2056 (1973).
¹⁷J. D. Garcia, *Phys. Rev. A* **1**, 280 (1970).
¹⁸J. M. Hansteen and O. P. Mosebekk, *Nucl. Phys.* **A201**, 541 (1973).
¹⁹M. Inokuti, *Rev. Mod. Phys.* **43**, 297 (1971).
²⁰L. Vriens, *Case Studies in Atomic Collisions*, edited by E. W. McDaniel and M. R. C. McDowell (North-Holland, Amsterdam, 1969), p. 335.
²¹H. Kolbenstvedt, *J. Appl. Phys.* **38**, 4785 (1967).
²²N. F. Mott and H. S. W. Massey, *The Theory of Atomic Collisions*, 3rd ed. (Oxford, New York, 1965), p. 110.
²³R. Anholt, *Phys. Rev. A* **19**, 1004 (1979).
²⁴J. D. Garcia, R. J. Fortner, and T. M. Kavanagh, *Rev. Mod. Phys.* **45**, 111 (1973).
²⁵J. F. Reading, A. L. Ford, and E. Fitchard, *Phys. Rev. Lett.* **36**, 573 (1976); A. L. Ford, E. Fitchard, and J. F. Reading, *Phys. Rev. A* **16**, 133 (1977).